

## Experimental determination of strength of pinned-joint carbon-epoxy laminate

Jan Krystek<sup>1</sup>, Lukáš Bek, Jan Bartošek, Robert Zemčík & Radek Kottner<sup>2</sup>

**Abstract:** This work focused on experimental determination of tensile strength of pinned-joint composite laminate. A composite material with high-strength carbon fibers and epoxy resin was used. Two different stacking configurations were analyzed. Digital image correlation technique was used for evaluation of displacement field around the pin. First failures were not obvious from dependences of tensile force and displacement. Since the first failure is accompanied by acoustic emission, therefore, the vibrations in the surroundings of the specimen were measured in addition. The force/displacement data, digital images and the vibration data were synchronized in time.

**Keywords:** Bearing; Composite; Digital image correlation; Displacement field

### 1. Introduction

The capability of pinned-joint strength prediction is an important part in mechanical engineering. Geometric parameters of joints influence their strengths [1, 2, 5]. Comparison between two stacking configurations in carbon-epoxy laminate ( $[0/-45/45/90]_s$  and  $[90/45/-45/0]_s$ ) was performed for hole diameter  $D = 6.35$  mm in [1, 2].

Assessment of first failure is very important for verification of numerical models for detection of failure of pinned-joint. Mostly, first failure cannot be revealed from the force/displacement curve. Therefore, the first failure was revealed from measuring of vibration. Displacement field was evaluated using digital image correlation (DIC) technique. Specimens with different geometric parameters and with different stacking configuration were tested in tension.

Typical failure mechanisms of the pinned-joint composite are shown in Fig. 1.

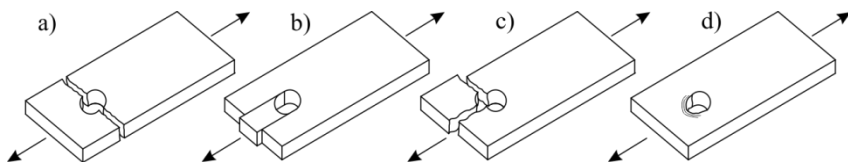


**Fig. 1.** Typical failure mechanism of pin joint a) net-tension, b) shear-out, c) mixed, d) bearing.

<sup>1</sup> Ing. Jan Krystek; Department of Mechanics, University of West Bohemia in Pilsen; Univerzitní 22, 306 14 Plzeň, Czech Republic; krystek@kme.zcu.cz

<sup>2</sup> Bc. Lukáš Bek; Ing. Jan Bartošek; Ing. Robert Zemčík, Ph.D.; Ing. Radek Kottner, Ph.D.; Department of Mechanics, University of West Bohemia in Pilsen; Univerzitní 22, 306 14 Plzeň, Czech Republic

## 2. Material and geometric properties of specimens

The specimens were cut using a water jet from carbon-epoxy laminates which were made from 8 pairs layers of prepreg. Pin holes were milled. The composite material consisted of Tenax HTS 5631 high-strength carbon fibres and epoxy resin. Identified mechanical properties of the composite material are presented in Table 1. The identification of the mechanical properties was carried out by means of tensile and compressive tests [3]. Therein, nonlinear function with constant asymptote [3] was used in identification process of shear modulus  $G_{12}$  in form

$$G_{12}(\gamma_{12}) = \frac{G_{12}^0}{\left[1 + \left(\frac{G_{12}^0 \cdot \gamma_{12}}{\tau_{12}^0}\right)^{n_{12}}\right]^{1 + \frac{1}{n_{12}}}}, \quad (1)$$

where  $G_{12}^0$  is the initial shear modulus,  $\gamma_{12}$  is the shear strain,  $\tau_{12}^0$  is the asymptote value of the shear stress and  $n_{12}$  is the shape parameter.

**Table 1.** Mechanical properties [3].

Linear model				Nonlinear model			Strength parameters					
$E_1$	$E_2$	$\nu_{12}$	$G_{12}$	$G_{12}^0$	$\tau_{12}^0$	$n_{12}$	$X^T$	$X^C$	$Y^T$	$Y^C$	$S^L$	$\alpha_0$
[GPa]	[GPa]	[-]	[GPa]	[GPa]	[GPa]	[-]	[MPa]	[MPa]	[MPa]	[MPa]	[MPa]	[°]
116.2	11.5	0.395	5.0	6.2	27.2	0.33	1800	850	55	213	82	57

Geometric parameters of the specimen are shown in Fig. 2, where  $D$  is the hole diameter,  $W$  is the width of the specimen,  $E$  is the distance from the centre of the hole to the free end,  $L$  is the distance from the centre of the hole to the fixed end,  $t$  is the thickness of the specimen.

Two different stacking configurations ( $[0/-45/45/90]_s$  and  $[90/45/-45/0]_s$ ) were tested in this work. Angles were measured from  $x$  axis. The hole diameter was  $D = 8$  mm, thickness  $t = 2.3$  mm, distance  $L = 90$  mm,  $E/D = \{1, 2, 3, 4, 5\}$ ,  $W/D = \{2, 3, 4, 5\}$ .

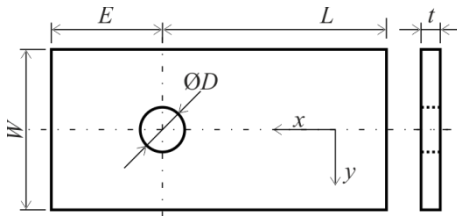


**Fig. 2.** Geometry parameters of specimen.

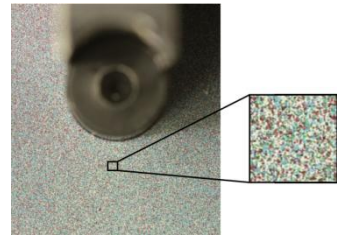


**Fig. 3.** Random color pattern on specimen

### 3. Experiments

Experimental setup is shown in Fig. 4. Specimens were tested in tension in the longitudinal direction. Zwick/Roell Z050 testing machine was used. The loading speed was  $v = 0.5$  mm/min.

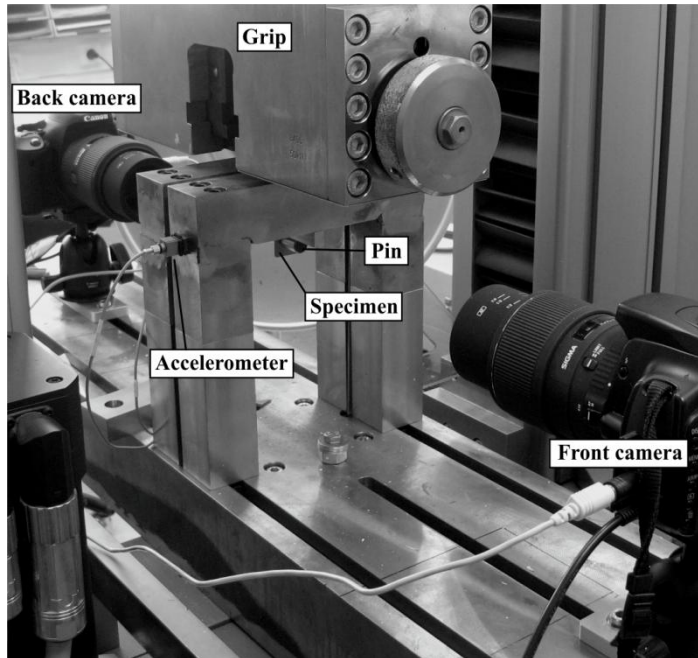
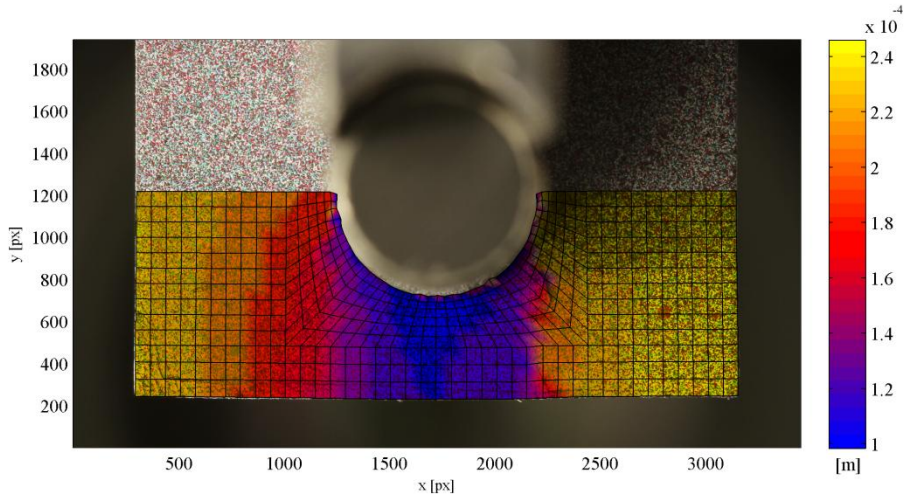


Fig. 4. Experimental setup.

It was not possible to use an extensometer in the setup, therefore, the method of digital image correlation [4, 6] was used for the evaluation of displacement field around the pin. A random high-contrast color pattern was applied on the surface of the specimen (Fig. 3). The specimen was monitored using two cameras during whole test including time before and after applied loading in regular time intervals ( $\Delta t = 3$  s). The positions of corresponding pixels in the two digitized images were compared, and thus, the in-plane displacement fields (Fig. 5) were obtained [6].

First failures were not obvious in the force/displacement curves (Fig. 6), therefore, an accelerometer was used for the measurement of vibrations. The location of the cameras results in the influence of the accelerometer record in the moment of mirror and shutter movement. The first failure was revealed from spectrogram using short-time Fourier transform. Force/displacement data, digital images and vibration record were synchronized in time. The synchronization was controlled by program which was created in the LabVIEW software.



**Fig. 5.** Displacement field around pin measured using DIC ( $D = 8$  mm,  $E/D = 1$ ,  $W/D = 3$ ,  $[0/-45/45/90]_s$ ).

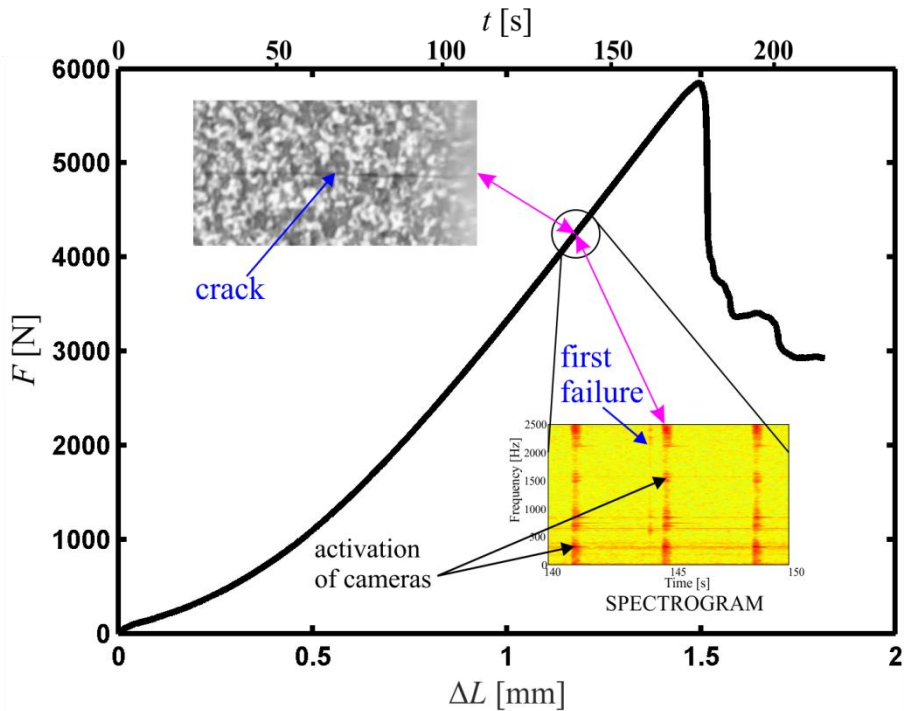


**Fig. 6.** Detection of first failure ( $D = 8$  mm,  $E/D = 3$ ,  $W/D = 2$ ,  $[90/45/-45/0]_s$ ).

## 4. Results

The influence of the ratio  $E/D$  on the specimen strength  $F_{\max}$  (Fig. 7 and Fig. 8) was significant only for  $E/D = 2$  for both tested stacking configurations. The maximum strength of the pinned-joint was reached for ratio  $E/D = 2$ . The bearing strength of the pinned-joint was decreasing with increasing ratio  $W/D$  (Fig. 9 and Fig. 10). Shear-out strength and net-tension strength depended significantly on the values of the geometric parameters of the joint. The net-tension failure mode occurred for ratio  $E/D = 1$  in case of  $[90/45/-45/0]_s$  laminate. Shear-out failure mode occurred for ratio  $E/D = 1$  in case of  $[0/-45/45/90]_s$  laminate. In all others cases, the bearing failure mode occurred. The minimum ratios were  $E/D = 2$ ,  $W/D = 2$  for  $[0/-45/45/90]_s$  laminate and  $E/D = 2$ ,  $W/D = 3$  for  $[90/45/-45/90]_s$  laminate. The bearing strength did not depend on the stacking configuration.

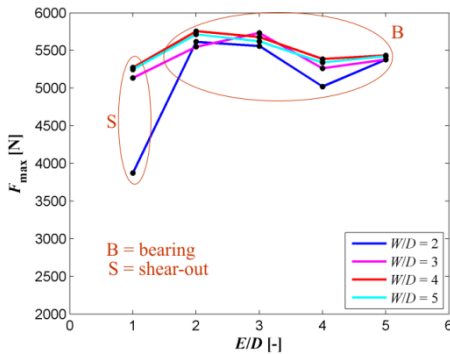


Fig. 7. Strength of pinned-joint  $[0/-45/45/90]_s$  laminate.

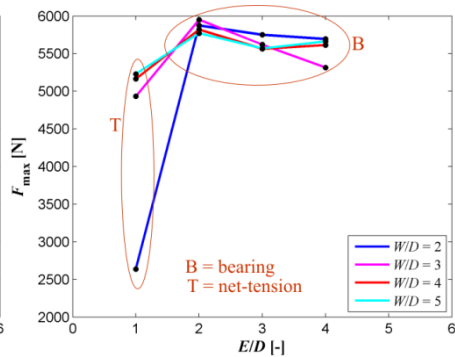


Fig. 8. Strength of pinned-joint  $[90/45/-45/0]_s$  laminate.

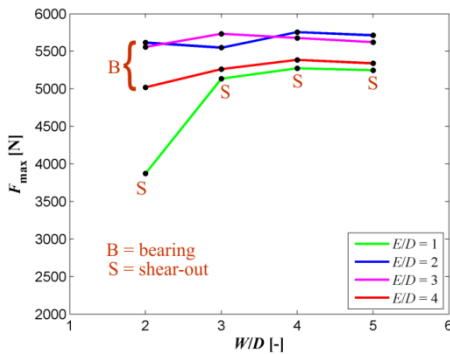


Fig. 9. Strength of pinned-joint  $[0/-45/45/90]_s$  laminate.

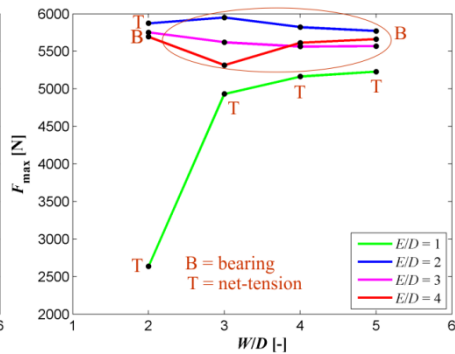


Fig. 10. Strength of pinned-joint  $[90/45/-45/0]_s$  laminate.

## 5. Conclusion

The experimental determination of the strength of pinned-joint composite laminate was performed in this work. The strength of pinned-joint was compared for two different stacking configurations. The evaluation of the displacement field was performed using the method of digital image correlation. Vibration around the specimen was measured for the analysis of the first failure. The first failure was determined from spectrogram using short-time Fourier transform.

In case of bearing failure mechanism ultimate failure did not occur. Therefore, for safety reasons, it can be advantageous to design pinned-joint geometry so that the bearing mode is induced. This can be achieved using the minimum ratios  $E/D$  and  $W/D$  obtained from the results. The bearing strength did not increase with increasing geometric ratios  $E/D$  and  $W/D$  and it was not dependent on stacking configuration.

## Acknowledgements

This work was supported by the European Regional Development Fund (ERDF), project "NTIS - New Technologies for Information Society", European Centre of Excellence, CZ.1.05/1.1.00/02.0090, project GACR P101/11/0288 and the project of Ministry of Education SGS-2010-046.

## References

- [1] Aktas A., "Bearing strength of carbon epoxy laminates under static and dynamic loading." *Composite Structures* 67 (2005), pp. 485-489. ISSN 0263-8223.
- [2] Aktas A., Dirikolu M. H., "An experimental and numerical investigation of strength characteristics of carbon-epoxy pinned-joint plates." *Composite Science and Technology* 64 (2004), pp. 1605-1611. ISSN 0266-3538.
- [3] Krystek J., Kroupa T. and Kottner R., "Identification of mechanical properties from tensile and compression tests of unidirectional carbon composite." In Proceedings: *48th International Scientific Conference: Experimental Stress Analysis 2010*, Palacky University, pp. 193-200, ISBN: 978-80-244-2533-7.
- [4] Sutton M.A., Ortu j.-J., Schreier H.W. *Image correlation for shape, motion and deformation measurements. Basic concepts, theory and applications*. Springer, 2009.
- [5] Yilmaz T, Sinmazcelik T., Effects of Geometric Parameters on Pin-bearing Strength of Glass/Polyphenylenesulphide Composites. *Journal of Composite Materials*. Vol. 43, No. 20/2009. ISSN 0021-9983.
- [6] Zemčík R., Boháč J., Kaiser J. and Plánička F., "Analysis of residual stresses in plastics using digital image correlation." In Proceedings: *49th International Scientific Conference: Experimental Stress Analysis 2011*, Brno University of Technology, pp. 435-439, ISBN: 978-80-214-4275-7.